


# *HYDIN* variants cause primary ciliary dyskinesia in the Finnish population

Thomas Burgoyne PhD<sup>1,2</sup> | Mahmoud R. Fassad PhD<sup>3,4</sup> | Rüdiger Schultz PhD<sup>5</sup> |  
Varpu Elenius PhD<sup>6</sup> | Jacqueline S. Y. Lim PhD<sup>3</sup> | Grace Freke PhD<sup>3</sup> |  
Ranjit Rai PhD<sup>2</sup> | Mai A. Mohammed PhD<sup>3,7</sup> | Hannah M. Mitchison PhD<sup>3</sup> |  
Anu I. Sironen PhD<sup>3,8</sup> 

<sup>1</sup>Institute of Ophthalmology, University College London, London, UK

<sup>2</sup>PCD Diagnostic Team and Department of Paediatric Respiratory Medicine, Royal Brompton Hospital, London, UK

<sup>3</sup>Great Ormond Street Institute of Child Health, University College London, London, UK

<sup>4</sup>Human Genetics Department, Medical Research Institute, Alexandria University, Alexandria, Egypt

<sup>5</sup>Allergy Centre, Tampere University Hospital, Tampere, Finland

<sup>6</sup>Department of Pediatrics, Turku University Hospital, University of Turku, Turku, Finland

<sup>7</sup>Biochemistry Department, Faculty of Science, Zagazig University, Zagazig, Egypt

<sup>8</sup>Natural Resources Institute Finland (Luke), Jokioinen, Finland

## Correspondence

Anu I. Sironen, PhD, Great Ormond St Institute of Child Health, University College London, 30 Guilford St, London, WC1N 1EH, UK.  
Email: [a.sironen@ucl.ac.uk](mailto:a.sironen@ucl.ac.uk)

## Funding information

Wellcome Trust Collaborative Award in Science; BEAT-PCD network; H2020 Marie Skłodowska-Curie Actions; Biotechnology and Biological Sciences Research Council; Ministry of Higher Education in Egypt; NIHR Great Ormond Street Hospital Biomedical Research Centre

## Abstract

**Introduction:** Primary ciliary dyskinesia (PCD) is a rare genetic disorder characterized by chronic respiratory tract infections and in some cases laterality defects and infertility. The symptoms of PCD are caused by malfunction of motile cilia, hair-like organelles protruding out of the cell. Thus far, disease causing variants in over 50 genes have been identified and these variants explain around 70% of all known cases. Population specific genetics underlying PCD has been reported highlighting the importance of characterizing gene variants in different populations for development of gene-based diagnostics and management.

**Methods:** Whole exome sequencing was used to identify disease causing variants in Finnish PCD cohort. The effect of the identified *HYDIN* variants on cilia structure and function was confirmed by high-speed video analysis, immunofluorescence and electron tomography.

**Results:** In this study, we identified three Finnish PCD patients carrying homozygous loss-of-function variants and one patient with compound heterozygous variants within *HYDIN*. The functional studies showed defects in the axonemal central pair complex. All patients had clinical PCD symptoms including chronic wet cough and recurrent airway infections, associated with mostly static airway cilia.

Hannah M. Mitchison and Anu I. Sironen are joint senior authors.

This is an open access article under the terms of the [Creative Commons Attribution](https://creativecommons.org/licenses/by/4.0/) License, which permits use, distribution and reproduction in any medium, provided the original work is properly cited.

© 2024 The Author(s). *Pediatric Pulmonology* published by Wiley Periodicals LLC.

**Conclusion:** Our results are consistent with the previously identified important role of *HYDIN* in the axonemal central pair complex and improve specific diagnostics of PCD in different national populations.

**KEYWORDS**

axoneme, diagnostics, *HYDIN*, motile cilia, PCD, variant

## 1 | INTRODUCTION

Primary ciliary dyskinesia (PCD) is an inherited disease where impairment of mucociliary clearance (MCC) leads to recurrent airway infections, bronchiectasis and in some cases progressively severe lung damage. The mucus accumulation in the airways is caused by malfunction of motile cilia. Other syndromic features in PCD are situs inversus, otitis media, hearing loss, complex congenital heart disease, and more rarely hydrocephalus and retinitis pigmentosa.<sup>1</sup> Furthermore, PCD variants may affect male and female fertility due to defective motile cilia in the oviduct and male efferent duct, and defects in sperm tail development. Motile cilia lining the airways remove mucus and pathogens by a forward beating pattern, which is disrupted by variants in genes regulating aspects of ciliogenesis or coding for dynein preassembly or structural proteins in motile cilia. Thus far variants in over 50 genes have been identified to cause PCD. The most commonly mutated genes code for components of the dynein arms, which are required for creating the movement of motile cilia.<sup>1,2</sup> The axonemal structure of motile cilia consists of 9+2 microtubules, inner and outer dynein arms, nexin links between the doublet microtubules, radial spokes connecting the outer microtubule doublets to the central pair and the central pair projection (Figure 1A).

The central pair projection is required for controlling the motility pattern created by the dynein arms and variants in central pair complex genes such as *HYDIN* have been shown to result in stiff and static cilia.<sup>3</sup> However, the central pair is not present in nodal cilia that govern left-right organ laterality and therefore variants in genes coding for central pair proteins do not cause situs inversus.<sup>4</sup> Recently, it has been shown that lack of *HYDIN* causes depletion of *SPEF2* from the ciliary central pair complex and thus immunostaining for *SPEF2* can be used as a diagnostic tool for PCD patients with *HYDIN* variants.<sup>5</sup> Variants in *SPEF2* mainly cause male infertility due to malformed and immotile sperm tails, and mild PCD symptoms have also been reported that affect the airways.<sup>6–8</sup>

Two highly similar copies of *HYDIN* are present in the human genome, *HYDIN* which is transcribed from chromosome 16 (hg38 16:70,802,084–71,230,722) and a paralogue pseudogene *HYDIN2*, which is located on chromosome 1 (hg38 1:146,547,367–146,898,974). *HYDIN2* appears to be mainly expressed in the brain and fetal tissues with low expression in the lung, due to a neuronal promoter.<sup>9</sup> *HYDIN2* is a duplicate of *HYDIN* exons 6–84 with short and long transcripts predicted to be transcribed, the most common isoform containing exons 6–19.<sup>9</sup> Due to their very high similarity, it is difficult to distinguish *HYDIN*-specific variants for diagnostics based

on short read DNA sequencing. We recently showed the ability for long read sequencing to overcome this challenge,<sup>10</sup> and here we investigate the potential to apply RNA sequencing of nasal brushing biopsies to confirm causality of *HYDIN* variants in PCD patients. In this study, we have identified novel and rare *HYDIN* variants in the Finnish population using exome and Sanger sequencing of DNA and RNA, and confirmed the functional effect of compound heterozygous variants using immunofluorescence and electron tomography.

## 2 | METHODS

### 2.1 | Subjects

Blood samples were collected for DNA extraction from 13 PCD patients, recruited at the University Hospitals of Turku, Kuopio and Tampere after written informed consent was given. Patients were selected for exome sequencing based on clinical symptoms underlining PCD; chronic airway and ear infections, low nasal nitric oxide (nNO) and abnormal cilia beating pattern. Gene panel results were negative for the selected patients. Nasal brushing samples were collected for high-speed video microscopy analysis (HSVA), electron microscopy, immunohistochemistry and gene expression studies when possible. The study was ethically approved by the University of Turku Ethics Committee (ETMK 69–2017), London Bloomsbury Research Ethics Committee approved by the Health Research Authority (08/H0713/82), and the referring hospitals.

### 2.2 | Nasal nitric oxide analysis

For nNO analysis, a CLD 88sp analyser equipped with a Denox 88 module for flow control was used with standard techniques (Eco Physics). If cooperativity was established, three consecutive trials were taken, from which the highest value was recorded. Nasal nitric oxide analysis was repeated on two different occasions.

### 2.3 | High-speed video microscopy analysis (HSVA)

Nasal epithelial cells were suspended in DMEM medium and evaluated under a differential-interference microscope (Zeiss) at x1000 magnification. Cilia beat was recorded with a digital high-speed video

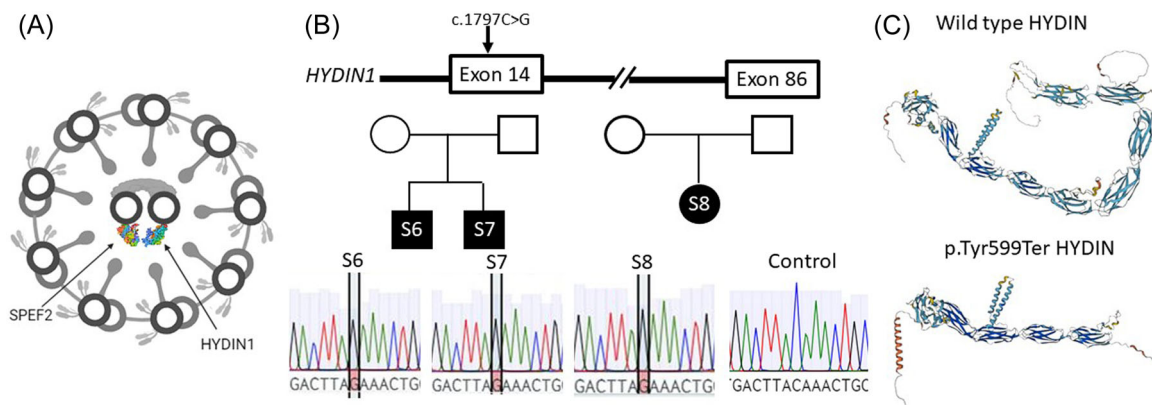


**FIGURE 1** Stop gain variants in *HYDIN* cause PCD in Finnish patients S6-S8. (A) *HYDIN* and *SPEF2* form a complex in the axonemal central pair projection. (B) Stop gain variant (c.1797 C > G) in *HYDIN* exon 14 was identified in three Finnish PCD patients and confirmed by Sanger sequencing. (C) The c.1797 C > G variant results in a predicted truncated *HYDIN* protein product as visualized by the AlphaFold protein structure prediction tool (<https://alphafold.ebi.ac.uk/>). PCD, primary ciliary dyskinesia.

(DHSV) camera (Hamamatsu Orca Flash 4.0) with a frame rate of 256 Hz. The detailed protocol for HSVA can be found in.<sup>11</sup> DHSV video sequences were played back frame by frame to determine the cilia beat frequency (CBF) by calculating the mean of all recorded cilia beat cycles. The cilia beating pattern (CBP) was determined by two independent expert operators. HSVA was repeated on two different occasions and averaged.

## 2.4 | Whole exome sequencing

The Nonacus Cell3 Exome panel was used for whole exome sequencing of patient DNA samples (<https://nonacus.com/cell3tm-target>). Unmapped reads were aligned to the current Human reference genome (GRCh38 build) by Burrows-Wheeler Aligner tool (Bwa-mem2 version) (Li and Durbin, 2010), SAM files were produced and indexed and converted to BAM format previous to marking and removing duplicates using Picard (<https://broadinstitute.github.io/picard/>). Subsequent analysis was executed following best practices guidelines for GATK from the Broad Institute (<https://gatk.broadinstitute.org/hc/en-us>). Firstly, base quality score recalibration (BQSR) was done to numerically correct individual base calls. Variant discovery was carried out in a two-step pipeline: variant calling with HaplotypeCaller followed by joint genotyping with GenotypeGVCFs. Once a multi-sample VCF file was obtained containing all definitive variant records, VariantRecalibrator was operated to fulfil Variant Quality Score Recalibration (VQSR) and refinement of the obtained variant callset.

Variants were individually selected for each sample. The called variants, including both single nucleotide variants (SNVs) and indels, were then annotated using ANNOVAR (<http://www.openbioinformatics.org/annovar/>). This tool enables functional annotation, and thus the final VCF files obtained contains detailed information for each variant site in the sample, such as their impact within a gene, predicted pathogenicity scores, minor allele frequency (MAF), zygosity status or reporting whether they have been recorded in large-scale databases like dbSNP.

## 2.5 | Variant prioritization

Variants were filtered for MAF < 1%, their predicted functional impact on the encoded protein (missense, splicing, frameshift or nonsense) and frequency (<0.001) in the Genome Aggregation Database (gnomAD, broadinstitute.org). A list of genes with high expression during motile cilia development ( $n = 652$ , reanalyzed gene list based on data in Marcet et al.<sup>12</sup>) was used to further filter variants in genes with potential roles in motile cilia. Finally, the pathogenicity of the identified variants was estimated using the Combined Annotation Dependent Depletion tool (CADD, <https://cadd.gs.washington.edu/snv>) with a CADD score >20 considered a significant pathogenicity score and associated softwares (Polyphen-2, SIFT, PROVEAN, AlphaFold). All variants were reported according to Human Genome Variation Society recommendations.<sup>13</sup> Variant pathogenicity was scored according to American College of Medical Genetics and Genomics and the Association for Molecular Pathology (ACMG-AMP) variant interpretation guidelines.<sup>14</sup> Due to the known inheritance pattern of PCD homozygous variants, these were prioritized, but output files were also analyzed for the presence of compound heterozygous variants.

## 2.6 | RNA extraction and RT-PCR

RNA was isolated from nasal brushing samples using a Qiagen RNeasy kit (Qiagen) and RNA was reverse-transcribed using a cDNA Reverse Transcription Kit (Applied Biosystems). cDNA was amplified using the TaqMan Fast Universal PCR Master Mix (Applied Biosystems). Primers used for RT-PCR are listed in Supplementary table 1.

## 2.7 | Sanger sequencing

The identified variants were confirmed in the probands and available family members by Sanger sequencing. Primers flanking the variant

were designed using the NCBI Primer-BLAST tool (Table S1). The genomic or cDNA sequence was amplified using standard PCR conditions and predicted primer annealing temperature. The specificity of the PCR product was confirmed on agarose gel and purified using ExoSAP-IT (Thermo Fisher Sci) for Sanger sequencing.

## 2.8 | Transmission electron microscopy and electron tomography

A nasal brush biopsy was collected from a patient using 0.6-mm bronchial cytology brush. The sample was fixed in 2.5% glutaraldehyde in cacodylate buffer before postfixing in 1% osmium tetroxide, and subsequently centrifuging in 2% agar to generate a pellet. Using increasing concentrations of ethanol followed by propylene oxide, the pellet was dehydrated before embedding in Araldite resin. 100 nm thick sections were cut and stained with 2% methanolic uranyl acetate and Reynolds lead citrate. Using a JEOL 1400+ transmission electron microscope (TEM) fitted with an AMT 16X CCD camera, conventional TEM images were acquired and 2D averaging was performed on TEM images using PCD-Detect.<sup>15</sup> To generate tomograms, perpendicular tilt series (dual axis) were collected using SerialEM (University of Colorado Boulder) with tilt increments of 1° over a range of ±60°. The tilt series were processed using IMOD<sup>16</sup> to generate a dual axis tomogram. Subtomographic averaging was performed in IMOD, averaging together the central pairs from eight cilia of patient S10 and from six cilia of a healthy control.

## 2.9 | Immunofluorescence

Respiratory epithelial ciliated cells from a nasal brushing of a PCD patient and a control sample were stained after blocking (10% BSA, in PBS) using DNAH5 (HPA037470, Cambridge Bioscience), RSPH4A (HPA031196, Sigma-Aldrich) and SPEF2 (HPA039606, Sigma-Aldrich) antibodies, colocalized with the cilia marker alpha-tubulin (322588, Invitrogen). After washes with PBST the slides were incubated with secondary antibodies Alexa Fluor 488 anti-mouse and Alexa Fluor 594 anti-rabbit (1:500). Slides were imaged using Zeiss Axio Observer 7 and deconvoluted using Huygens Deconvolution software (<https://svi.nl/Huygens-Deconvolution>).

## 3 | RESULTS

### 3.1 | HYDIN variants identified in the Finnish population

Whole exome sequencing of Finnish PCD patients with chronic respiratory infections and otitis media (Table 1) identified one homozygous variant (NM\_001270974:exon14:c.1797 C > G:p. Tyr599Ter, pathogenic) in three patients and two heterozygous variants (NM\_001270974:exon80:c.13801delG:p. Glu4601ArgfsTer17, pathogenic and NM\_001270974:exon76:c.12899 G > C:p. Cys4300Ser, likely pathogenic) in one patient. These variants had a low frequency in the gnomAD database and were predicted pathogenic or likely pathogenic, in keeping with ACMG/AMP guidelines,<sup>14</sup> using Polyphen, Sift and Provean, also having high CADD scores (Table 2). The homozygous variants were identified in two nonconsanguineous families and were confirmed using *HYDIN* specific primers for Sanger sequencing of patient DNA (Figure 1B). This variant results in a stop gain in exon 14 and a predicted truncated protein product that would severely disrupt *HYDIN* function. The protein 3D structure prediction tool AlphaFold (<https://alphafold.ebi.ac.uk/>) was used to demonstrate the effect of the stop gain variant on protein structure, showing a clear reduction in size and a lack of several protein domains (Figure 1C).

WES of patient S10 showed 4 variants within the *HYDIN* coding region of which two were predicted to be likely pathogenic (Table 2). A frameshift deletion (c.13801delG) was identified in exon 80 in cis with a missense SNV (c.13800 G > C). In trans with this allele, another nonsynonymous SNV was found in exon 76 (c.12899 G > C), which was predicted to be damaging by Polyphen, Sift and Provean with a CADD score of 23.8 (Table 2). An additional benign nonsynonymous SNV was detected in exon 22 (c.3291 A > G).

### 3.2 | HYDIN variants confirmed by sanger sequencing and RNA expression

The stop gain variants were confirmed by Sanger sequencing of patients DNA using *HYDIN* specific primers (Table S1, Figure 1B). The similarity of *HYDIN* and *HYDIN2* across exons 72 to 85 hindered the

**TABLE 1** Patient characteristics of four patients with mutations in the *HYDIN* gene.

Patient ID	Ethnicity	DOB	Sex	CBF Hz	Cilia beating pattern (HSVA)	nNO (nl/min)	Clinical symptoms
S10	Finnish	1998	F	-	Unsynchronized, wavy	15	Recurrent sinusitis, otitis, respiratory infections, bronchiectasis
S6	Finnish	2005	M	10.8	Stiff, static	29	Recurrent sinusitis, otitis, respiratory infections
S7	Finnish	1999	M	0	Stiff, static	23	Recurrent sinusitis, otitis, respiratory infections
S8	Finnish	1999	F	0	Static	5	Recurrent sinusitis, otitis, respiratory infections, bronchiectasis

Abbreviation: CBF, cilia beat frequency

**TABLE 2** *HYDIN* variants identified in Finnish PCD patients.

Patient ID	Gene	Function	Variant	rsID	Zygotyzy	Frequency GenomAD	CADD score
S10	<i>HYDIN</i>	Frameshift deletion	<i>HYDIN</i> :NM_001270974:exon80: c.13801delG:p. Glu4601ArgfsTer17	rs752405406	het	0.00002478	33
S10		Missense	<i>HYDIN</i> :NM_001270974:exon80: c.13800 G > C:p. Lys4600Asn	rs751812896	het	0.00005122	16
S10	<i>HYDIN</i>	Missense	<i>HYDIN</i> :NM_001270974:exon76: c.12899 G > C:p. Cys4300Ser	rs200169224	het	0.001577	23.8
S10	<i>HYDIN</i>	Missense	<i>HYDIN</i> :NM_001270974:exon22: c.3291 A > G:p. Ile1097Met	rs183427172	het	0.00367	5.758
S6	<i>HYDIN</i>	Stop gain	<i>HYDIN</i> :NM_001270974:exon14: c.1797 C > G:p. Tyr599Ter	rs760517494	hom	0.0001524	35
S7	<i>HYDIN</i>	Stop gain	<i>HYDIN</i> :NM_001270974:exon14: c.1797 C > G:p. Tyr599Ter	rs760517494	hom	0.0001524	35
S8	<i>HYDIN</i>	Stop gain	<i>HYDIN</i> :NM_001270974:exon14: c.1797 C > G:p. Tyr599Ter	rs760517494	hom	0.0001524	35

Abbreviation: PCD, primary ciliary dyskinesia.

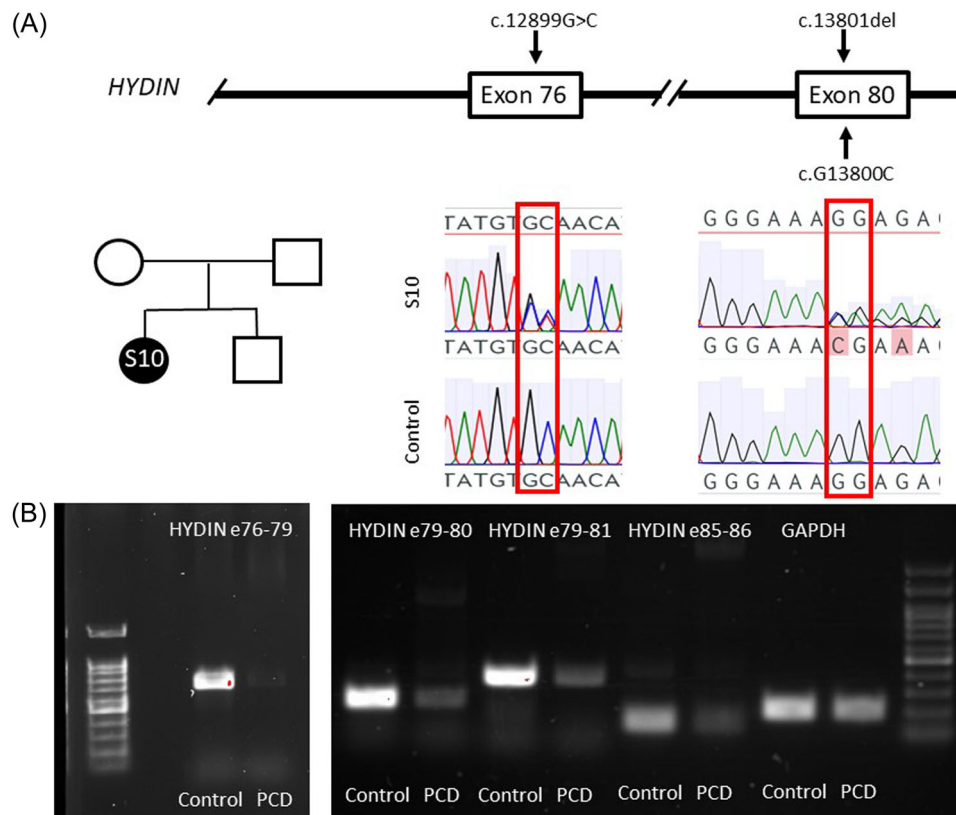


**FIGURE 2** Compound heterozygous variants result in decreased *HYDIN* expression in a PCD patient S10. (A) Sanger sequencing of patient RNA confirmed heterozygosity of the identified pathogenic *HYDIN* variants. (B) *HYDIN* transcript expression was decreased in the patient with *HYDIN* variants c.12899 G > C and c.13801delG compared to control. *GAPDH* was used as a loading control. PCD, primary ciliary dyskinesia.

confirmation of the identified variants in patient S10 since no *HYDIN* specific DNA primers could be designed. Therefore, we extracted RNA from the patient and her mother for transcript sequencing to confirm the variants for which we failed to find *HYDIN* specific

primers for DNA sequencing. Sequencing of the variants at RNA level confirmed the presence and heterozygosity of both potentially causative *HYDIN* variants in the patient (Figure 2A) and the mother was confirmed as a carrier of variant c.12899 G > C. Sanger

sequencing also showed a variant c.12900 C > T predicted to result in a nonsynonymous SNV (Figure 2A), which did not affect the protein sequence. Therefore, we conclude that the PCD in patient S10 may likely be caused by variants c.13801delG and c.12899 G > C. Furthermore, *HYDIN* expression across exons 76–81 and at the end of the gene across exons 85–86 was dramatically decreased compared to the control (Figure 2B).

### 3.3 | The axonemal central pair structure is affected in a patient with compound heterozygous *HYDIN* variants

To further validate the causality of the heterozygous *HYDIN* variants we investigated the structural defects in the ciliary axoneme of the patient's nasal sample. TEM showed an apparently normal microtubular organization in the ciliary axonemes and the presence of dynein arms (Figure 3A), which was also confirmed by positive immunostaining with outer dynein arm component DNAH5 (Figure 4A). Furthermore, the radial spokes appeared unaffected as demonstrated by the presence of the radial spoke component RSPH4A (Figure 4A). Electron tomography has been demonstrated as a useful tool for identification of central pair structural defects<sup>17</sup> and thus we utilized

this method to confirm the expected disruption of the central pair complex arising from *HYDIN* variants. Tomograms showed a lack of the proximal projection of the central pair complex in the patient with compound heterozygous variants p. Glu4601Argfs\*17 and p. Cys4300Ser (Figure 3C), which was not obvious by the conventional TEM (Figure 3A). PCD-Detect<sup>15</sup> was also able to identify the central pair defect in the patient compared to control (Figure 3D) demonstrating the usefulness of this tool in diagnostics. Since it has previously been shown that *HYDIN* is required for localization of *SPEF2* in the axonemal central pair projection<sup>5</sup> we used *SPEF2* immunostaining to confirm the lack of the *HYDIN/SPEF2* protein complex in the axonemal central pair. *SPEF2* was localized along the whole length of cilia in airway epithelial cells from a healthy control individual, but was completely depleted in the patient's cilia (Figure 3B).

Furthermore, we screened for the presence of the identified causative variants and protein localizations in the nasal sample of the mother of the patient. Localizations of *SPEF2*, *DNAH5* and *RSPH4A* were comparable to a control sample (Figure 4B). Sequencing of the *HYDIN* variants showed inheritance of the c.12899 G > C variant from the mother (Figure 4C). These results strongly support the conclusion that the identified *HYDIN* variants in patient S10 are causative for PCD and confirm the deleterious effect of the variants on *HYDIN* localization to the ciliary axoneme.

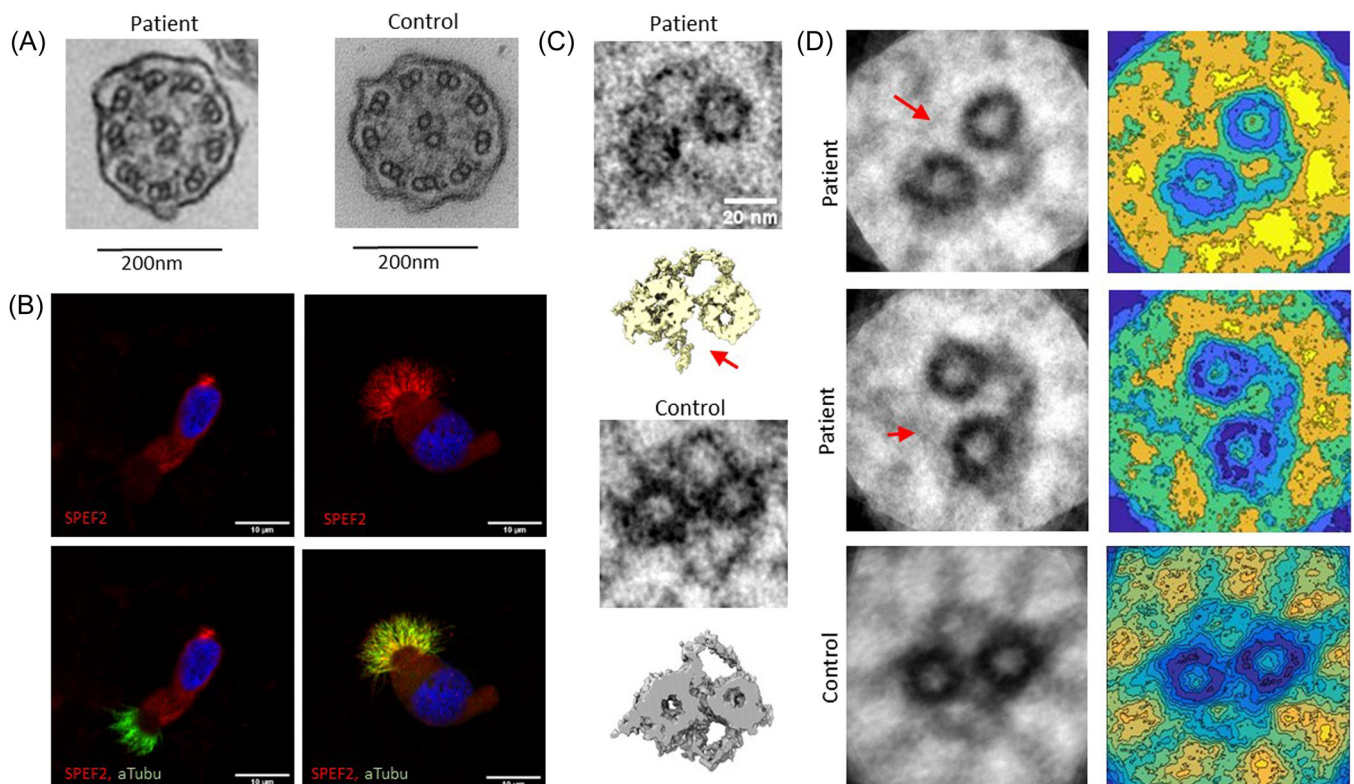


**FIGURE 3** The axonemal central pair projection is affected in the PCD patient S10 with compound heterozygous *HYDIN* variants. (A) TEM showed apparently normal microtubular structure and the presence of dynein arms and radial spokes in the patient's axonemal cross sections. (B) *SPEF2* staining was depleted in cilia of the patient's nasal brushing samples. (C) Electron tomography showed a lack of the *SPEF2/HYDIN* complex in the patient's central pair projection. (D) 2D image averaging using PCD Detect identified the lack of the *SPEF2/HYDIN* complex in the patient's central pair. PCD, primary ciliary dyskinesia.

### 3.4 | *HYDIN* variants cause stiff cilia motility in Finnish PCD patients

Patients S6, S7 and S8 who carry the homozygous stop gain *HYDIN* variants all showed almost static, extremely stiff cilia in their airway epithelial cell samples, which is in line with previous studies of patients with *HYDIN* variants (Table 1). Patient S10 with heterozygous *HYDIN* variants had stiff cilia with some unsynchronized movement, which may be due to residual *HYDIN* in some of the axonemal central pair projections (Table 1). All patients were reported to have low NO and recurrent sinusitis and otitis (Table 1). No situs inversus was reported for any of the patients as is expected for individuals carrying *HYDIN* variants based on the lack of central pair structure in nodal cilia. Patients S8 and S10 had developed bronchiectasis. We conclude that the symptoms reported for the patients can be explained by the

identified *HYDIN* variants and that this information can be used for genetic counselling and management of PCD in these patients.

## 4 | DISCUSSION

Although genetic variants for PCD have been identified in over 50 genes across the world, the genetics of PCD is population specific in many cases; the majority of identified variants causing PCD are found in small number of patients. However, more widespread variants have been identified within populations and across different ethnicities and geographical populations.<sup>2,18–20</sup> Thus, it is important to identify the population specific variants to improve diagnostics and management of the disease. Identification of genetic causes of a disease enables better prediction of the evolution of symptoms in

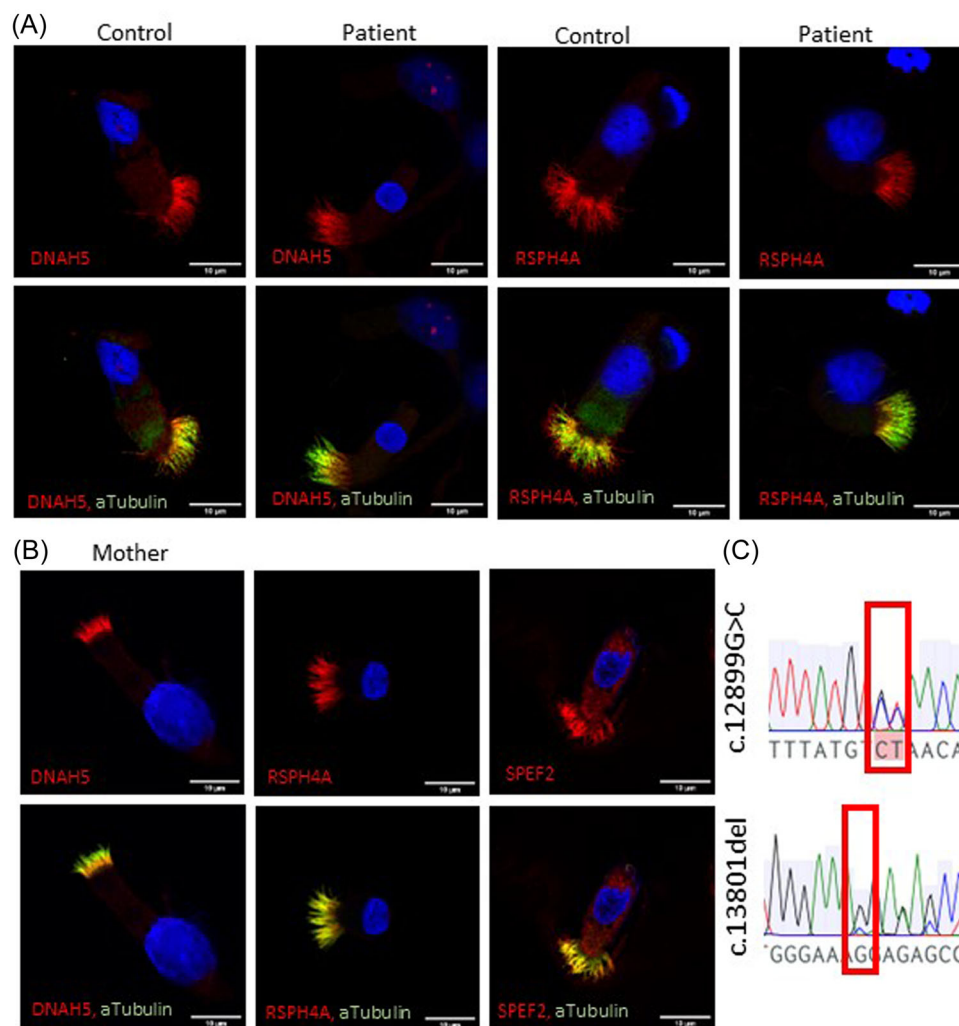


**FIGURE 4** Immunofluorescence confirmed the presence of the main axonemal structures and Sanger sequencing the inheritance pattern for one *HYDIN* variant in patient S10. (A) Outer dynein arm protein DNAH5 and radial spoke protein RSPH4A protein localization in PCD patient with c.12899 G > C and c.13801delG variants was comparable to the control. (B) SPEF2, DNAH5 and RSPH4A were present in the airway cilia of the patient's carrier mother. (C) Sanger sequencing of patients mother showed heterozygosity of variant c.12899 G > C and control homozygosity of variant c.13801delG confirming the inheritance of c.12899 G > C from the mother to the patient. PCD, primary ciliary dyskinesia.

each patient and development of treatments, including personalised medicines to improve their quality of life.

There is tissue specificity and different severity of disease progression depending on the genes affected and types of variants in PCD, hence the need for better understanding of its genetic causes at the population level. The most severe PCD phenotypes arise from genes affecting multiciliogenesis (*CCNO*, *MCIDAS*) due to either complete lack or an inefficiently low number of motile cilia in the airways. Although these genes do not affect sperm tail formation, they may affect fertility via a lack of efferent duct cilia.<sup>21,22</sup> Genotype-phenotype relationships have also been identified in large-scale topological data analysis.<sup>1,23</sup> PCD disease severity also appears to be significantly worse in patients with variants in the molecular ruler genes *CCDC39* and *CCDC40* compared to most other structural gene variants in PCD, whilst other variants introducing more subtle axonemal defects include those in *DNAH11*.

*HYDIN* variants are relatively common in PCD patients,<sup>3,10,24</sup> although clinical diagnosis of these patients has been hindered due to a lack of clear structural changes in the axoneme, lack of situs inversus and a pseudogene hindering the sequence-based diagnostics. *HYDIN* is a large gene containing 86 exons and spanning more than 423 kb and due to development of methods to improve diagnostics of patients with *HYDIN* variants recent studies have identified *HYDIN* as a common cause of PCD in many populations; 8.7% of cases in Quebec cohort<sup>24</sup> and 7% in UK cohort. For identification of *HYDIN* variants in the UK cohort Fleming et al developed long-read sequencing to overcome the issues with the *HYDIN2* pseudogene sequence.<sup>10</sup> Furthermore, electron tomography and immunofluorescence microscopy have provided tools to confirm the structural defect in patients with *HYDIN* variants and demonstrating the loss of *HYDIN* at the central pair complex through SPEF2 staining. PCD Detect has been developed based on image averaging and enhancement as a diagnostic tool kit to assess cases which are difficult to diagnose, but have a suggestive HSVA result, TEM result, or a variant of unknown significance.<sup>15</sup> In this study we utilized PCD Detect and structural studies to confirm the causality of compound heterozygous variants together with immunofluorescence and RNA experiments.

In Finland genetic variants in PCD patients have previously been identified only in the *DNAH11* and *CFAP300* genes.<sup>3,11,25</sup> The *HYDIN* variants identified in this study contribute to the understanding of the genetic background of PCD in Finland and enable development of genetics diagnostics within the Finnish population.

Confirmation of the causality of *HYDIN* variants is complicated by the presence of the pseudogene *HYDIN2*. Here we have utilized RNA sequencing and electron tomography to confirm the compound heterozygous variants in *HYDIN*, which couldn't be verified with Sanger sequencing of DNA or by conventional TEM. The homozygous stop gain variant c.1797 C > G was found in three PCD patients and is predicted to truncate the protein product by 4522 aa, which likely causes degradation of the protein by nonsense mediated decay (NMD). The variant is not present in the GenomAD database and based on the results of this study we concluded that this is the disease-causing variant in these patients.

The compound heterozygous variants in patient S10 were validated with RNA expression and sequencing, immunohistochemistry and EM tomography and the results showed convincing evidence that PCD is caused by *HYDIN* defects in this patient as well. The c.13801delG (rs752405406) variant is enriched in the Finnish population with an allele frequency of 0.0005309, and is specific to the European population (0.000001695). The c.12899 G > C (rs200169224) variant is more common in the Finnish population (0.003242), but can also be found in European, African and American populations (0.0002078–0.001935). Thus, these variants can be expected to be a more common cause of PCD in the Finnish population.

Our study has shown that *HYDIN* variants explain 31% of the analysed cases (4/13, three families) in the Finnish patient cohort. Other recurrent PCD-causing variants were previously reported in *CFAP300* (three families) and *DNAH11* (two families).<sup>11,25</sup> There is still work to be done to establish a more complete gene panel for genetic diagnostics in Finland, but several Finnish population enriched variants have been identified thus far and this information can be used for improving clinical diagnostics for PCD.

#### AUTHOR CONTRIBUTIONS

Thomas Burgoyne produced the electron tomography images and analysed the sample with PCD-detect. Mahmoud R. Fassad performed the variant calling. Rüdiger Schultz collected patient samples. Varpu Elenius collected clinical data, patient samples and performed HSVA. Jacqueline S. Y. Lim performed immunofluorescence staining. Grace Freke performed Sanger sequencing. Ranjit Rai prepared electron microscopy samples. Mai A. Mohammed extracted RNA. Hannah M. Mitchison supervised the study. Anu I. Sironen wrote the manuscript, conducted imaging, Sanger sequencing, variant filtering and bioinformatic analysis. All authors contributed corrections and improvements to the manuscript.

#### ACKNOWLEDGMENTS

The authors would like to acknowledge the funding for this research from BBSRC grant BB/V011251/1. Anu I Sironen was also funded by Marie Skłodowska-Curie individual fellowship No. 800556 from the European Union's Horizon 2020 Research and Innovation Programme. Hannah M. Mitchison was supported by NIHR GOSH BRC, Ministry of Higher Education in Egypt and acknowledges support from the BEAT-PCD network (COST Action 1407 and European Respiratory Society (ERS) Clinical Research Collaboration). Mahmoud R. Fassad was supported by a Wellcome Trust Collaborative Award in Science (210585/Z/18/Z).

#### CONFLICT OF INTEREST STATEMENT

The authors declare no conflict of interest.

#### DATA AVAILABILITY STATEMENT

The data that support the findings of this study are available from the corresponding author, (Anu I Sironen), upon reasonable request.

#### ORCID

Anu I. Sironen  <http://orcid.org/0000-0003-2064-6960>



## REFERENCES

- Shoemark A, Rubbo B, Legendre M, et al. Topological data analysis reveals genotype-phenotype relationships in primary ciliary dyskinesia. *Eur Respir J*. 2021;58(2):2002359.
- Fassad MR, Patel MP, Shoemark A, et al. Clinical utility of NGS diagnosis and disease stratification in a multiethnic primary ciliary dyskinesia cohort. *J Med Genet*. 2020;57(5):322-330.
- Olbrich H, Schmidts M, Werner C, et al. Recessive HYDIN mutations cause primary ciliary dyskinesia without randomization of left-right body asymmetry. *Am J Hum Genet*. 2012;91(4):672-684.
- Best S, Shoemark A, Rubbo B, et al. Risk factors for situs defects and congenital heart disease in primary ciliary dyskinesia. *Thorax*. 2019;74(2):203-205.
- Cindrić S, Dougherty GW, Olbrich H, et al. SPEF2- and HYDIN-mutant cilia lack the central pair-associated protein SPEF2, aiding primary ciliary dyskinesia diagnostics. *Am J Respir Cell Mol Biol*. 2020;62(3):382-396.
- Liu C, Lv M, He X, et al. Homozygous mutations in SPEF2 induce multiple morphological abnormalities of the sperm flagella and male infertility. *J Med Genet*. 2020;57(1):31-37.
- Liu W, Sha Y, Li Y, et al. Loss-of-function mutations in SPEF2 cause multiple morphological abnormalities of the sperm flagella (MMAF). *J Med Genet*. 2019;56(10):678-684.
- Mori M, Kido T, Sakamoto N, et al. Novel SPEF2 variant in a Japanese patient with primary ciliary dyskinesia: a case report and literature review. *J Clin Med*. 2022;12(1):317.
- Dougherty ML, Nuttle X, Penn O, et al. The birth of a human-specific neural gene by incomplete duplication and gene fusion. *Genome Biol*. 2017;18(1):49.
- Fleming A, Galey M, Briggs L, et al. Combined approaches, including long-read sequencing, address the diagnostic challenge of HYDIN in primary ciliary dyskinesia. *Eur J Human Genet*. 2024;32:1074-1085.
- Schultz R, Elenius V, Fassad MR, et al. CFAP300 mutation causing primary ciliary dyskinesia in Finland. *Front Genet*. 2022;13:985227.
- Marcet B, Chevalier B, Luxardi G, Coraux C, Zaragosi LE, Cibois M et al. Control of vertebrate multiciliogenesis by miR-449 through direct repression of the Delta/Notch pathway. *Nat Cell Biol*. 2011;13(6):693-699. doi:10.1038/ncb2241
- den Dunnen JT, Dalgleish R, Maglott DR, et al. HGVS recommendations for the description of sequence variants: 2016 update. *Hum Mutat*. 2016;37(6):564-569.
- Richards S, Aziz N, Bale S, et al. Standards and guidelines for the interpretation of sequence variants: a joint consensus recommendation of the American college of medical genetics and genomics and the association for molecular pathology. *Genet Med*. 2015;17(5):405-424.
- Shoemark A, Pinto AL, Patel MP, et al. PCD detect: enhancing ciliary features through image averaging and classification. *Am J Physiol Lung Cell Mol Physiol*. 2020;319(6):L1048-L1060.
- Kremer JR, Mastrorarde DN, McIntosh JR. Computer visualization of three-dimensional image data using IMOD. *J Struct Biol*. 1996;116(1):71-76.
- Shoemark A, Burgoyne T, Kwan R, et al. Primary ciliary dyskinesia with normal ultrastructure: three-dimensional tomography detects absence of DNAH11. *Eur Respir J*. 2018;51(2):1701809. doi:10.1183/13993003.13901809-13992017
- Hannah WB, Seifert BA, Truty R, et al. The global prevalence and ethnic heterogeneity of primary ciliary dyskinesia gene variants: a genetic database analysis. *Lancet Respir Med*. 2022;10(5):459-468.
- Rumman N, Fassad MR, Driessens C, et al. The Palestinian primary ciliary dyskinesia population: first results of the diagnostic and genetic spectrum. *ERJ Open Res*. 2023;9(2):00714-2022.
- Xu Y, Feng G, Yano T, et al. Characteristic genetic spectrum of primary ciliary dyskinesia in Japanese patients and global ethnic heterogeneity: population-based genomic variation database analysis. *J Hum Genet*. 2023;68(7):455-461.
- Hoque M, Kim EN, Chen D, Li FQ, Takemaru KI. Essential roles of efferent duct multicilia in male fertility. *Cells*. 2022;11(3):341.
- Terré B, Lewis M, Gil-Gómez G, et al. Defects in efferent duct multiciliogenesis underlie male infertility in GEMC1-, MCIDAS- or CCNO-deficient mice. *Development*. 2019;146(8):dev162628. doi:10.1242/dev.162628
- Berger LM, Cancian M, Meyer DR. Maternal re-partnering and new-partner fertility: associations with nonresident father investments in children. *Child Youth Serv Rev*. 2012;34(2):426-436.
- Shapiro AJ, Sillon G, D'Agostino D, et al. HYDIN variants are a common cause of primary ciliary dyskinesia in French Canadians. *Ann Am Thorac Soc*. 2023;20(1):140-144.
- Schultz R, Elenius V, Lukkarinen H, Saarela T. Two novel mutations in the DNAH11 gene in primary ciliary dyskinesia (CILD7) with considerable variety in the clinical and beating cilia phenotype. *BMC Med Genet*. 2020;21(1):237.

## SUPPORTING INFORMATION

Additional supporting information can be found online in the Supporting Information section at the end of this article.

**How to cite this article:** Burgoyne T, Fassad MR, Schultz R, et al. *HYDIN* variants cause primary ciliary dyskinesia in the Finnish population. *Pediatr Pulmonol*. 2024;59:3601-3609. doi:10.1002/ppul.27267